Research Article

Selected Paper from the 6th International Thai Institute of Chemical Engineering and Applied Science Conference (ITIChE2016)

Fire-retardant Paper Based on Montmorillonite and Oil Palm Trunk Fibres

Saowapa Chotisuwan*, Kreepon Wannarit, Phetcharapon Kaewna, Sareena Kardae, Yupadee Chaisuksan and Jareerat Roumcharoen
Department of Science, Faculty of Science and Technology, Prince of Songkla University, Pattani Campus, Pattani, Thailand

* Corresponding author. E-mail: saowapa.c@psu.ac.th DOI: 10.14416/j.ijast.2018.11.002
Received: 24 July 2017; Revised: 17 October 2017; Accepted: 18 October 2017; Published online: 8 November 2018

Abstract
Fire-retardant paper was prepared by mixing of Montmorillonite (MTM), Carboxymethyl Cellulose (CMC) and Cellulose Fibres (CF) isolated from oil palm trunk biomass by alkaline treatment. The mixtures of dispersed CMC, MTM and CF with various ratios were stirred for 24 h, then casted and dried to form paper. The samples were characterized by Fourier transform infrared spectroscopy (FT-IR), X-ray diffraction (XRD), Scanning Electron Microscopy (SEM) and Thermogravimetric Analysis (TGA). Their mechanical and fire retardance properties were also evaluated. The CMC50 : MTM50 paper with CF (12 phr) was the proper ratio according to the good of flame-retardant testing and maximum tensile testing at 24.7 MPa and Young's Modulus at 13.7 MPa.

Keywords: Fire-retardant paper, Montmorillonite, Cellulose fibres, Carboxymethyl cellulose

1 Introduction

Large number of biomass from oil palm agriculture such as oil palm trunk (more than 20–30 years old of oil palm trees) can be used as cellulose source rather than soil amendment or fertilizer. The main chemical composition of oil palm trunk biomass consists of cellulose (up to 41%), hemicellulose, and lignin [1]. Cellulose structure contains linear glucose homopolymer bonded together with β-(1→4)-linked glucopyranose units with high degree of polymerization (DP), about 10,000. The hydroxyl groups in cellulose structure form hydrogen bond between cellulose fibres and also with oxygen of nearby molecules resulting in cellulose reactivity and physical properties [2]. Consequently, Cellulose Fibres (CF) have been reported to be used as biocompatibility materials in medical applications [3], templating materials in functionalization nanocomposites [4], reinforcing fibres in polypropylene/cellulose composites [5], and binding agent in clay nanopaper composites as fire-retardant paper [4]. Pyrolysis of pure cellulose is observed rapidly at 325–365°C with little char residues [6], [7]. Charring formation can act as oxygen barrier. Addition of fire retardants such as some inorganic chemicals is possible to inhibit or retard some stages of combustion process. Fire retardant mechanism composes of physical and chemical mechanisms. Physical mechanism for fire inhibition can be proceeded by thermal insulation containing protective layer, dilution of gases, and energy absorption. Chemical mechanism composes of addition of flame inhibitors by controlling the decomposing reactions, protection against afterglowing, and combination of inhibitors [8]. The ideal of fire retardant is the pyrolytic processes emitted only carbon or char and water [8].

Clay mineral such as Montmorillonite (MTM) has been reported to mix with cellulose and Carboxymethyl Cellulose (CMC) to form fire-retardant and ductile clay nanopaper [7]. CMC and cellulose can disperse and intercalate into MTM structure. MTM is 2 : 1 layer-type

Please cite this article as: S. Chotisuwan, K. Wannarit, P. Kaewna, S. Kardae, Y. Chaisuksan, and J. Roumcharoen, "Fire-retardant paper based on montmorillonite and oil palm trunk fibres," *Applied Science and Engineering Progress*, vol. 12, no. 4, pp. 277–285, Oct.–Dec. 2019.

clay composed of two silicate tetrahedrally coordinated sheets surrounding a sandwiched octahedrally coordinated sheet of aluminum ions. It also acts as thermal insulator due to low thermal conduction and gas barrier properties, and also improves mechanical property of hybrid paper [7], [9].

The aim of this work was to extract Cellulose Fibres (CF) from oil palm trunk biomass by alkaline pretreatment and to prepare the fire-retardant paper by mixing the CF with MTM and CMC colloidal dispersions using casting technique. The chemical, physical including mechanical properties and morphology of the clay paper biocomposites were characterized by various techniques as well as vertical flame-retardant testing.

2 Experimental

2.1 *Materials*

Oil palm (*Elaeis guineensis Jacq*.) trunk biomass (OPTF) was collected from oil palm plantation at Klong Kanan subdistrict, Nuea Khlong district, Krabi province, Thailand. All AR grade chemicals (except Ca-MTM, $Ca(ClO)_2$ and CMC) in this work were used as received.

2.2 *Extraction of cellulose fibres from oil palm trunk fibres*

Dried oil palm trunk fibres were prehydrolyzed with 2 wt% sodium hydroxide solution in an autoclave at pressure 15 lb_f/in^2 for 1 h, then followed by bleaching with 3 wt% calcium hypochlorite solution. Then acid hydrolysis was carried out with 5 wt% oxalic acid solution in an autoclave at pressure 5 lb_f/in^2 for 1 h. Cellulose fibres were filtered through 0.45 μm Nylon filter and dried in hot air oven at 50°C. Extracted cellulose fibres were dispersed in distilled water to obtain 1 wt% CF to use as a CF source for paper preparation. Chemical compositions of the raw oil palm trunk fibres and extracted CF were analyzed according to ASTM method including ASTM D1103-60 for alpha cellulose and ASTM D1104-56 for lignin.

2.3 *Preparation of fire-retardant paper biocomposites*

The 1 wt% CMC and 1 wt% MTM dispersions were prepared in distilled water before mixing together with various weight ratios of CMC and MTM (10 : 90, 20 : 80, 30 : 70, 40 : 60, and 50 : 50). The mixtures were stirred for 24 h and ultrasonicated for 15 min, then poured into mold and dried in hot air oven at 50°C for 18–20 h. The CMC50 : MTM50 ratio was mixed with various CF phr (part per hundred) at 4, 8, and 12 phr to form paper biocomposites. All samples were kept in dessicator prior to characterization.

2.4 *Characterization of fire-retardant paper*

The chemical and physical properties of the CMC : MTM and CMC : MTM : CF samples were characterized by various techniques as follows.

2.4.1 Fourier transform infrared spectroscopy (FT-IR)

Untreated oil palm fibres, extracted CF, CMC, MTM, and hybrid paper were scanned by FT-IR spectrometer (Tensor 27 spectrometer, BRUKER) using Attenuated Total Reflectance (ATR) technique in the range of 400–4,000 cm^{-1} with 32 scans at a resolution of 4 cm^{-1}.

2.4.2 X-ray diffraction (XRD)

XRD patterns of untreated oil palm trunk fibres, extracted CF, CMC, MTM, and hybrid paper were recorded by X-ray diffractometer (Model X'Pert MPD, Philips, the Netherlands) equipped with Cu Kα (1.54 Å) XRD tube with current 30 mA and 40 kV. The diffraction intensity was detected at the 2θ range of 5–50° with step scan of 0.6°.min^{-1}. The Crystallinity Index (CI) was approximately calculated by the following Equation (1) [10].

$$CI = \frac{(I_{002} - I_{am})}{I_{002}} \times 100 \quad (1)$$

Where I_{002} is the XRD intensity at (002) crystal lattice or at 2θ between 22° and 24° and I_{am} is the XRD signal at 2θ nearly 18°.

2.4.3 Scanning Electron Microscopy (SEM)

Surface and cross-sectional morphology of hybrid paper samples were observed by scanning electron microscope (Model JSM-5800 LV, JEOL, Japan) operating at 20 kV. The samples were deposited on carbon tape mounted on sample stubs and coated with

gold using sputtering technique.

2.4.4 Thermogravimetric analysis (TGA)

TGA of untreated oil palm trunk fibres, extracted CF, CMC, MTM, and hybrid paper were observed by thermogravimetric analyzer (Model TGA7, Perkin Elmer, USA). The TGA data were recorded in oxygen environment from 40 to 800°C at heating rate of 10°C.min^{-1}.

2.4.5 Tensile testing

Tensile stress and Young's modulus of the hybrid paper (1 × 10 cm specimen size) was performed by Tensile Tester (H10KS, Hounsfield test machine) equipped with a 0.4 N load cell with the strain rate of 4 mm.min^{-1}.

2.4.6 Flame-retardant testing

In this work, self-extinguishing flammability testing of paper biocomposites was performed [11]. Ten replications of vertical specimen (1 cm × 6 cm) were exposed to a flame ignited from Bunsen burner for 1 s. Afterglow phenomenon including afterglow time and residue were observed.

3 Results and Discussion

3.1 *Physicochemical property of extracted CF*

Untreated oil palm trunk fibres in this work contained 40.4 ± 1.0% alpha cellulose, 23.0 ± 1.0% hemicellulose, 18.7 ± 1.1% lignin, and 5.6 ± 0.3% extractives (dry weight). Alpha cellulose of extracted CF samples after pretreated with 2 wt% NaOH and bleached with 3 wt% $Ca(ClO)_2$ solutions and finally acid hydrolysis with oxalic acid solution in an autoclave increased to 94.0 ± 0.2% dry weight with traces of lignin (0.7 ± 0.1%).

From the XRD result in Figure 1(a), untreated oil palm fibres showed broad XRD peak around 2θ values of 16° and 22° corresponding to $(1\bar{1}0)$ and (002) lattice plan representing cellulose I crystal form, and not cellulose II [12]. Broad peak at 18° also indicated amorphous materials in untreated oil palm fibres [10]. After cellulose fibre isolation by alkaline pretreatment

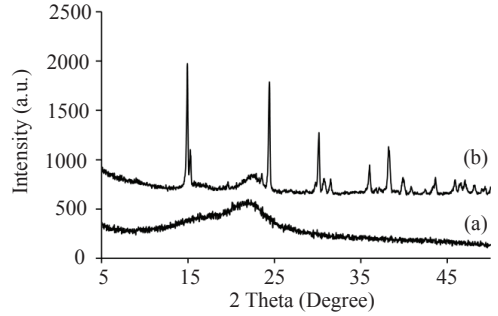

Figure 1: X-ray patterns of (a) raw and (b) extracted CF.

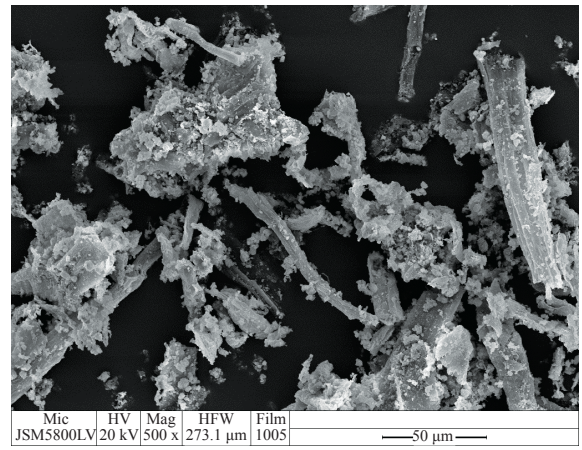

Figure 2: SEM images of extracted CF.

in an autoclave, bleaching and acid hydrolysis, the extracted CF showed the main XRD sharp signal at 2θ values of 14.9°, 24.4°, and 30° while broad XRD at 22° still observed. It is clearly indicated that crystallinity of cellulose I increases after extraction process. The Crystallinity Index (CI) of raw oil palm fibres calculated by Segal equation was about 29%. The CI of extracted CF increased to 90% due to hemicellulose and lignin removal by alkaline pretreatment, bleaching, and acid hydrolysis. The extracted fibres were in the form of cellulose I_β which was predominant form in wood [13]. Crystallinity of the extracted CF in this work was higher than that of cellulose nanocrystals isolated from oil palm trunk with acid hydrolysis method incorporating with ethanol/toluene pre-extraction and sodium chlorite bleaching [14].

Figure 2 represented SEM image of extracted CF consisting of cellulose crystals and microfibrils with 4–20 µm diameter and 30–160 µm length. However,

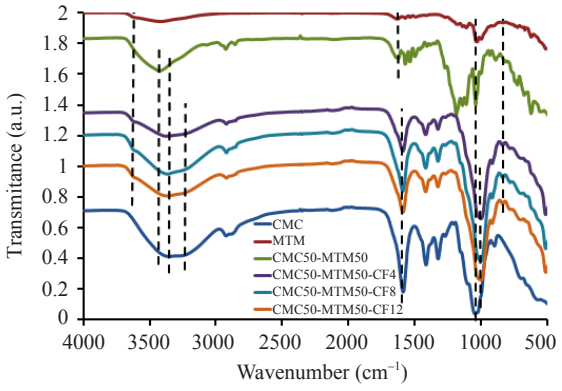

Figure 3: FT-IR spectra of CMC, MTM, and CMC50 : MTM50 with/without CF (4, 8 and 12 phr).

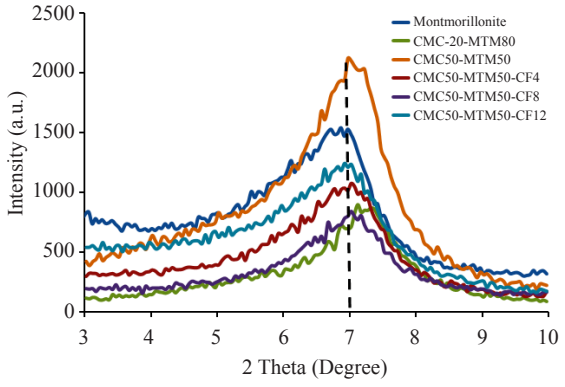

Figure 4: X-ray patterns of MTM, various ratios of CMC : MTM, and CMC50 : MTM50 with CF (4, 8, and 12 phr).

the aspect ratio (length : diameter) around 10 of these extracted CF was lower than cellulose nanocrystals isolated from oil palm trunk using acid hydrolysis method (aspect ratio around 45) [14]. These extracted CF samples were expected to show interaction with MTM to form fire-retardant paper biocomposites.

3.2 *Effect of CF on physicochemical property of CMC/MTM hybrid paper*

The interaction between CMC, MTM and CF was characterized by FT-IR spectroscopy. The hydroxyl groups of CF and CMC were observed at wavenumber around 3640–3300 cm^{-1} (Figure 3). FT-IR peak at 3611 cm^{-1} represented -OH stretching of MTM [15]. Broad FT-IR spectra centered at 3414 and 3364 cm^{-1} represented interlayer O-H stretching (hydrogen bonding) between hydroxyl groups of MTM and CMC, respectively [15]. It was observed that FT-IR peak centered at 3244 cm^{-1} for paper biocomposites decreased and slightly shift to lower wavenumber inferred the interaction between hydroxyl groups of CMC-MTM-CF. The FT-IR peak at 1634 cm^{-1} assigned to O-H bending of absorbed water of MTM. This FT-IR peak assigned to O-H bending of absorbed water of CMC50 : MTM50 was increased compared with bare MTM possibly due to MTM layers preferred to locate on the surface of paper. After mixing with CF, this peak was merged with carboxyl groups (-C=O) at 1593 cm^{-1}.

The sharp FT-IR peak at 1593 cm^{-1} assigned to asymmetric carboxyl groups (-C=O) stretching of CMC [15]. These peak slightly decreased for paper biocomposites but higher than that of CMC50 : MTM50 indicating that CMC and MTM were well dispersion with addition of CF. After mixing CMC and MTM at ratio of 50 : 50 with CF (4, 8, and 12 phr), hydrogen bonding still observed at broad peak at wavenumber 3640 cm^{-1} [6]. The wavenumber at 1053–1020 cm^{-1} assigning to Si-O-Si stretching of MTM was observed at 1041 cm^{-1}. However, after mixing MTM with CMC, this peak was merged with C-O-C pyranose ring stretching vibration of CMC [15]. FT-IR absorption of paper biocomposites was also observed at 840 cm^{-1} corresponding to the Al-O-C bond [6]. This peak may represent hydrogen bonding between hydroxyl group of CF and Al-O of MTM platelet surface [6]. This signal was very weak; thus this interaction was not strong indicated that lacking of intercalation in these paper biocomposites.

The effect of additional CF was characterized by XRD as shown in Figure 4. The diffraction peak of MTM at 2θ around 6.9° slightly shift to 7.1° after mixing with CMC indicating aggregation of MTM platelets due to electronegative surface of MTM. Addition of CF (4, 8, and 12 phr) also shifted XRD peaks to 7° indicating that CF was not sufficient to intercalate into all MTM layers. The distances (d, nm) between MTM layers were calculated by Bragg's equation. The *d* distance of MTM slightly decreased from 1.5 nm to 1.3 nm. However, increasing amount of CF in hybrid paper (4–12 phr) did not significantly change the distance between MTM layers as the data from Figure 4 and Table 1.

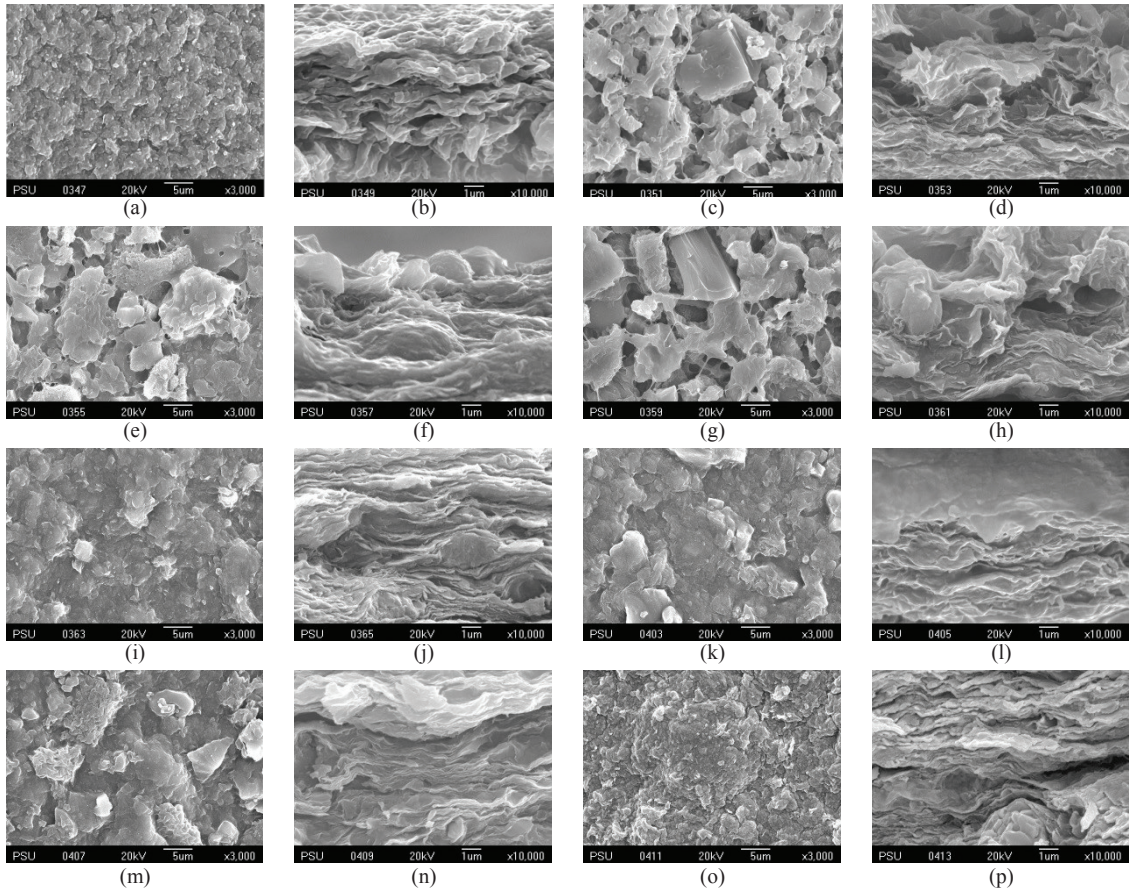

Figure 5: SEM images of (a) CMC10 : MTM90, (b) cross section of CMC10 : MTM90, (c) CMC20 : MTM80, (d) cross section of CMC20 : MTM80, (e) CMC30 : MTM70, (f) cross section of CMC30 : MTM70, (g) CMC40 : MTM60, (h) cross section of CMC40 : MTM60, (i) CMC50 : MTM50, (j) cross section of CMC50 : MTM50, (k) CMC50 : MTM50 : CF4, (l) cross section of CMC50 : MTM50 : CF4, (m) CMC50 : MTM50 : CF8, (n) cross section of CMC50 : MTM50 : CF8, (o) CMC50 : MTM50 : CF12, and (p) cross section of CMC50 : MTM50 : CF12 samples.

Table 1: Tensile strength and Young's modulus of the samples

Samples	Distance between MTM Layers; d (nm)	Tensile Strength (MPa)	Young's Modulus (MPa)
MTM	1.29	-	-
CMC50 : MTM50	1.27	26.8	18.3
CMC50 : MTM50 : CF4	1.24	16.8	11.9
CMC50 : MTM50 : CF8	1.25	23.7	13.0
CMC50 : MTM50 : CF12	1.27	24.7	13.7

However, according to Liu and Berglund [7], the d distance of MTM layers increased from 1.26 to 1.80 nm after mixing with Na-CMC and CF due to good dispersion of CF into Na-MTM galleries. Surface of MTM platelets have permanently negative charges and the MTM edge contains negative and positive charges as amphoteric edge sites depend on the pH value, for example, at pH 6.5, MTM have a neutral net charge [16]. CMC is an anionic linear polysaccharide containing numerous hydroxyl and carboxylic groups [17], thus its negative charges might be adsorbed onto the edge of MTM rather than MTM surface. Surface and cross section images of the CMC : MTM with and without CF were observed by SEM as shown in Figure 5.

MTM samples composed of two silicate sheets surrounding with a sandwiched coordinated sheet of alumina to form platelet-shape and layers. CMC

completely dissolve in water forming clear film after drying but it is also electronegative surface. This possibly caused to hardly form well dispersion of CMC and MTM in the samples as shown in Figure 5. Increasing CMC contents from 10 to 40 wt% resulted in inhomogeneous surface of hybrid samples with MTM platelets. The MTM platelets are electronegative surface resulting in swelling in aqueous medium. However, degree of aggregation of MTM platelets increases if the salinity of the system increases [18]. Since the CMC structure composes of carboxyl groups (-COOH), CMC can form bond with cations such as Na^+ and especially Ca^{2+} of MTM. Small amounts of CMC (10–40 wt%) were not sufficient to interact with MTM through cation-carboxyl bond forming some self-aggregation of MTM. However, cross sections of the CMC : MTM (CMC contents from 10 to 40 wt%) samples presented nonuniform layer structure with a scale around 100 nm. These MTM layers preferred orientation parallel to the sample surface with wavy appearance or low range order in cross sectional plane. Increasing CMC contents from 10 to 40 wt% also resulted in decreasing the distance between the layers of MTM and slightly increasing uniform layer structure. Electrostatic or hydrogen bonding interaction between MCM and CMC leads to multilayer formation. It was found from Figure 5 that CMC50 : MTM50 sample with 40–50 μm thickness showed smooth surface at 5 μm scale indicating well dispersion of both species or better interaction between CMC and MTM of paper than other CMC : MTM ratios. Thus CMC50 : MTM50 ratio was chosen further to mix with CF (4, 8, and 12 phr). The CF and CMC samples were interacted with MTM, they also dispersed on MTM surface and possibly inserted between MTM layers. However, small amounts of CF were not sufficient to complete intercalation of all MTM platelets. Moreover, diameter of extracted CF was not in nanoscale thus the fibres might not have good interact with MTM.

Cross section of each CMC50 : MTM50 and CMC50 : MTM50 with CF samples in Figure 5 also showed MTM layers with 2–45 nm distance between layers. Increasing the amount of CF resulted in small decreasing of the distance between MTM layers due to interaction between CF and MTM layers. In this work, addition of CF in CMC50 : MTM50 samples did not improve tensile strength and Young's modulus of the samples possibly due to previous reasons. The CMC50 : MTM50 : CF12 paper gave maximum tensile testing at 24.7 MPa and Young's Modulus at 13.7 MPa, lower than those of CMC50 : MTM50 samples (26.8 MPa and 18.3 MPa, respectively). The mechanical properties in this work were much lower than those compared to other work [6], [7] using nanocellulose due to lower aspect ratio of cellulose. Nanocellulose with high aspect ratio showed good interaction with MTM even there was not complete intercalation into all MTM platelets.

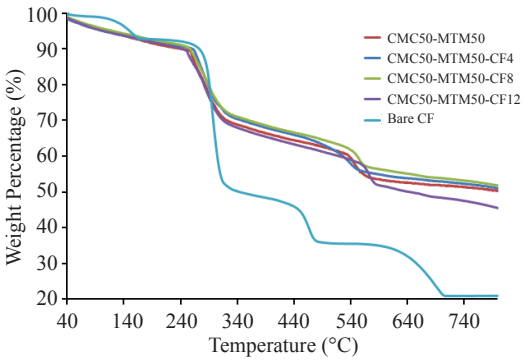

Figure 6: TGA curves of CF, CMC50-MTM50 and CMC50-MTM50-CF samples.

Thermal property of samples was characterized by TGA analysis in oxygen atmosphere as shown in Figure 6 and Table 2. The TGA results in Figure 6 showed three main decomposition stages consisting moisture decomposition (around 40–70°C), CMC and alpha cellulose decomposition or thermal cracking stage (around 260–300°C) [6]. The carbonization of CMC and alpha cellulose was normally decomposed at 440–500°C [6], [7]. The last decomposition stage of CF was observed at around 600°C. However, due to the interaction between CMC-CF-MTM and MTM layers of hybrid surface, the decomposition part of CF (T_{max2S}) at 480–500°C was shifted to 560–590°C. The degradation rates of CF in hybrid samples were slower than bare CF samples. According to SEM images in Figure 5, surface of paper samples mostly contained MTM platelets which had low thermal conductivity, low oxygen transport, resulting in slow burning of CMC and CF.

Moreover, decomposition products possibly diffused slowly through MTM layers [9]. The total residue at 800°C of CMC50 : MTM50, CMC50 : MTM50 : CF4 and CMC50 : MTM50 : CF8

was not significant difference (around 50% total residue), whereas the residue of CMC50 : MTM50 : CF12 decreased to 45%.

However, from Table 2, increasing amount of CF to 12 phr can significantly increase T_{max2} to 573°C due to high charring formation and thermal shielding. Thus, CMC50 : MTM50 : CF12 paper should be the proper ratio to give the good self-extinguishing flammability test.

Table 2: TGA data of CF, CMC, CMC50-MTM50 and CMC50-MTM50-CF samples in oxygen gas

Samples	$T_{onset\ 10\%}$ (°C)	T_{max1} (°C)	T_{max2} (°C)	Total Residue at 800°C (%)
CMC	90	268	449	16
CF	273	297	467	21
MTM	98	99	627	82
CMC50 : MTM50	258	282	535	50
CMC50 : MTM50 : CF4	237	270	504	51
CMC50 : MTM50 : CF8	260	285	556	52
CMC50 : MTM50 : CF12	251	280	573	45

3.3 *Fire-retardant property of CMC/MTM/CF hybrid paper*

The results for fire-retardant testing of CMC50 : MTM50 and CMC50 : MTM50 : CF (4–12 phr) samples after vertical burning in flame by Bunsen burner for 1 s are shown in Figure 7. Afterglow phenomenon, char length, and residues were also observed as shown in Table 3.

Table 3: Flammability data of CMC50-MTM50 and CMC50-MTM50-CF samples

Samples	Char length (cm)	Residue (wt% of Total Mass)
CMC50 : MTM50	0.30	96
CMC50 : MTM50 : CF4	0.24	96
CMC50 : MTM50 : CF8	0.14	95
CMC50 : MTM50 : CF12	0.10	95

The MTM layers in hybrid paper were thermal insulator while CMC and CF burned quickly in air. Figure 7 showed charring formation after vertical fire-retardant testing, all the samples did not completely burn. After removal of Bunsen burner flame from CMC50 : MTM50 and CMC50 : MTM50 : CF (4–8 phr) samples, the flame was extinguish within a few second. For CMC50 : MTM50 : CF (12 phr) sample, the flame was extinguish and then flameless combustion or red glowing was observed. Thus, char length of CMC50 : MTM50 : CF (12 phr) was shorter than others while the residue (wt% of total mass) was not significantly different. Thermal decomposition of CMC and CF released char and water. Charring formation and released water inhibited oxygen permeation resulting in fire-retardant property of the samples [7]. These thermal shielding can slow increase in temperature of sample lead to self-extinguish flammability property [11]. However, oxygen permeability and cone calorimetry of the CMC : MTM hybrid paper with small amount of cellulose should be further characterized as well as improved the paper making process to obtain long range order of MTM layers and good interaction between CF, CMC, and MTM.

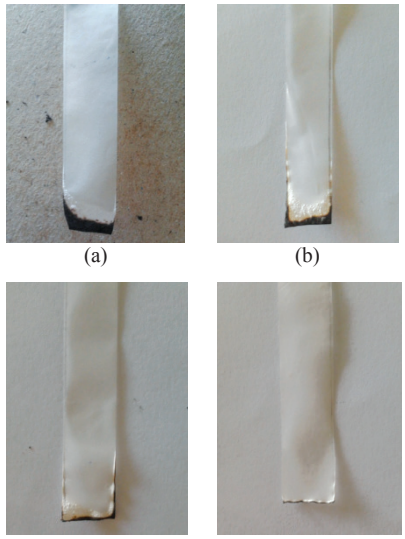

Figure 7: Fire-retardant of samples after burning in flame for 1 sec (a) CMC50 : MTM50, (b) CMC50 : MTM50 : CF4, (c) CMC50 : MTM50 : CF8, and (d) CMC50 : MTM50 : CF12.

4 Conclusions

Cellulose fibres extracted from oil palm trunk biomass by alkaline treatment were mixed with various ratios of CMC and MTM in the colloidal aqueous phase to form 40–50 μm thickness paper. The CMC50 :

MTM50 sample showed surface preferable of MTM layers and smoother surface of paper than other ratios. The CMC50 : MTM50 : CF with 12 phr paper was the proper ratio according to good fire-retardant property due to low thermal conductivity, low oxygen diffusion of MTM layers, and charring formation of CMC and CF after vertical burning testing.

Acknowledgments

This work has been supported by the government budget of Prince of Songkla University (SAT590164S). The authors would like to convey special appreciation to the academic committee of The 6th International Thai Institute of Chemical Engineering and Applied Science Conference (ITIChE2016) for providing the opportunity for this work to be published in this journal.

References

[1] R. Sun and J. Tomkinson, "Fractional separation and physico-chemical analysis of lignins from the black liquor of oil palm trunk fibre pulping," *Separation and Purification Technology*, vol. 24, pp. 529–539, Sep. 2001.

[2] A. Kaushik and M. Singh, "Isolation and characterization of cellulose nanofibrils from wheat straw using steam explosion coupled with high shear homogenization," *Carbohydrate Research*, vol. 346, pp. 76–85, Jan. 2011.

[3] B. M. Cherian, A. L. Leão, S. F. de Souza, L. M. M. Costa, G. M. de Olyveira, M. Kottaisamy, E. R. Nagarajan, and S. Thomas, "Cellulose nanocomposites with nanofibres isolated from pineapple leaf fibers for medical applications," *Carbohydrate Polymers*, vol. 86, no. 4, pp. 1790–1798, Oct. 2011.

[4] V. Nagy, K. Halász, M.-T. Carayon, I. A. Gural'skiy, S. Tricard, G. Molnár, A. Bousseksou, L. Salmon, and L. Csóka, "Cellulose fiber nanocomposites displaying spin-crossover properties," *Colloids and Surfaces A: Physicochemical and Engineering Aspects*, vol. 456, pp. 35–40, Aug. 2014.

[5] S. Thanomchat, K. Srikulkit, B. Suksut, and A. K. Schlarb "Morphology and crystallization of polypropylene/microfibrillated cellulose composites," *International Journal of Applied Science and Technology*, vol. 7, no. 4, pp. 23–34, Oct. 2014.

[6] A. Liu, A. Walther, O. Ikkala, L. Belova, and L. A. Berglund, "Clay nanopaper with tough cellulose nanofiber matrix for fire retardancy and gas barrier functions," *Biomacromolecules*, vol. 12, no. 3, pp. 633–641, Mar. 2011.

[7] A. Liu and L. A. Berglund, "Fire-retardant and ductile clay nanopaper biocomposites based on montmorrilonite in matrix of cellulose nanofibers and carboxymethyl cellulose," *European Polymer Journal*, vol. 49, pp. 940–949, Apr. 2013.

[8] E. Bohmer, "Thermal Properties," in *Handbook of Physical Testing of Paper*, 2nd ed., New York: Marcel Dekker, 2002, pp. 419–420.

[9] J. Zhuge, J. Gou, R.-H. Chen, A. Gordon, J. Kapat, D. Hart, and C. Ibeh, "Fire retardant evaluation of carbon nanofiber/graphite nanoplatelets nanopaper-based coating under different heat fluxes," *Composites: Part B*, vol. 43, pp. 3293–3305, Dec. 2012.

[10] L. Segal, J. J. Creely, A. E. Martin, and C. M. Conrad, "An empirical method for estimating the degree of crystallinity of native cellulose using the X-ray diffractometer," *Textile Research Journal*, vol. 29, no. 10, pp. 786–794, Oct. 1959.

[11] F. Carosio, J. Kochumalayil, F. Cuttica, G. Camino, and L. Berglund, "Oriented clay nanopaper from biobased components-mechanisms for superior fire protection properties," *Applied Materials and Interfaces*, vol. 7, pp. 5847–5856, Mar. 2015.

[12] M. Wada, L. Heux, and J. Sugiyama, "Poly morphism of cellulose I family: Reinvestigation of cellulose IVI," *Biomacro-molecules*, vol. 5, pp. 1385–1391, Jul. 2004.

[13] Y. Nishiyama, P. Langan, and H. Chanzy, "Crystal structure and hydrogen-bonding system in cellulose I_β from synchrotron X-ray and neutron fiber diffraction," *Journal of the American Chemical Society*, vol. 124, no. 31, pp. 9074–9082, Aug. 2002.

[14] J. Lamaming, R. Hashim, O. Sulaiman, C. P. Leh, T. Sugimoto, and N. A. Nordin, "Cellulose nanocrystals isolated from oil palm trunk," *Carbohydrate Polymers*, vol. 127, pp. 202–208, Aug. 2015.

[15] M. Ul-Islam, T. Khan, J. K. Park, "Nano reinforced bacterial cellulose-montmorillonite composites for biomedical applications," *Carbohydrate Polymers*, vol. 89, pp. 1189–1197, Aug. 2012.

[16] Y. Song, D. A. Hagen, S. Qin, K. M. Holder, K. Falke, and J. C. Grunlan, "Edge charge neutralization of clay for improved oxygen gas barrier in multilayer nanobrick wall thin films," *ACS Applied Materials & Interfaces*, vol. 8, no. 50, pp. 3478–3479, Nov. 2016.

[17] W. Tongdeesoontorn, L. J. Mauer, S. Wongruong, P. Sriburi, and P. Rachtanapun, "Effect of carboxymethyl cellulose concentrationon physical properties of biodegradable cassava starch-based films," *Chemistry Central Journal*, vol. 5, no. 1, pp. 1–8, 2011.

[18] S. Abend and G. Lagaly, "Sol–gel transitions of sodium montmorillonite dispersions," *Applied Clay Science*, vol. 16, pp. 201–227, Mar. 2000.